



Københavns Universitet



## Decoherence in Nearly-Isolated Quantum Dots

Folk, J.; Marcus, Charles M.; Harris jr, J.

*Published in:*  
Physical Review Letters

*DOI:*  
[10.1103/PhysRevLett.87.206802](https://doi.org/10.1103/PhysRevLett.87.206802)

*Publication date:*  
2000

*Citation for published version (APA):*  
Folk, J., M. Marcus, C., & Harris jr, J. (2000). Decoherence in Nearly-Isolated Quantum Dots. Physical Review Letters, 87(20), 2066802. <https://doi.org/10.1103/PhysRevLett.87.206802>

# Decoherence in Nearly-Isolated Quantum Dots

J. A. Folk,<sup>1</sup> C. M. Marcus,<sup>1,2</sup> and J. S. Harris, Jr.<sup>3</sup>

<sup>1</sup>*Department of Physics, Stanford University, Stanford, California 94305*

<sup>2</sup>*Department of Physics, Harvard University, Cambridge, Massachusetts 02138*

<sup>3</sup>*Department of Electrical Engineering, Stanford University, Stanford, California 94305*

Decoherence in nearly-isolated *GaAs* quantum dots is investigated using the change in average Coulomb blockade peak height upon breaking time-reversal symmetry. The normalized change in average peak height approaches the predicted universal value of 1/4 at temperatures well below the single-particle level spacing,  $T < \Delta$ , but is greatly suppressed for  $T > \Delta$ , suggesting that inelastic scattering or other dephasing mechanisms dominate in this regime.

The study of quantum coherence in small electronic systems has been the subject of intense theoretical and experimental attention in the last few years, motivated both by questions of fundamental scientific interest concerning sources of decoherence in materials [1, 2, 3, 4, 5], as well as by the possibility of using solid state electronic devices to store and manipulate quantum information [6, 7].

Taking advantage of quantum coherence in the solid state requires a means of isolating the device from various sources of decoherence, including coupling to electronic reservoirs. In this context, we have investigated coherent electron transport through quantum dots weakly coupled to reservoirs via tunneling point-contact leads. In this nearly-isolated regime, it is expected theoretically that inelastic relaxation due to e-e interactions will vanish below a temperature that is parametrically larger than the mean quantum level spacing in the dot,  $\Delta$  [8, 9, 10].

It is not obvious, however, how to measure coherence in nearly-isolated electronic structures. In this Letter, we introduce a novel method, applicable in this regime, that uses the change in average Coulomb blockade (CB) peak height upon breaking time-reversal symmetry as the metric of quantum coherence within the dot. By comparing our data to a model of CB transport that includes both elastic and inelastic transport processes [11], we find inelastic rates that are consistent with dephasing rates  $\tau_\phi^{-1}$  in open quantum dots measured using ballistic weak localization [4]. Extracting precise values for inelastic scattering rates using this method appears possible, but would require a quantitative theory of the crossover from elastic to inelastic tunneling [12].

When a quantum dot is connected to reservoirs (labeled 1,2) via leads with weak tunneling conductance,  $g_{1,2} \ll 1$  (in units of  $e^2/h$ ), transport is dominated by Coulomb blockade, which suppresses conduction except at specific voltages on a nearby gate. The result is a series of evenly-spaced, narrow conduction peaks as the gate voltage is swept, as seen in Fig. 1. In this regime, the usual techniques for extracting electron decoherence from transport measurements, for instance using weak localization [13, 14], are not applicable. Instead, we take advantage of an analog of weak localization that reflects a sensitivity of the spatial statistics of wave functions to the breaking of time-reversal symmetry. As in con-

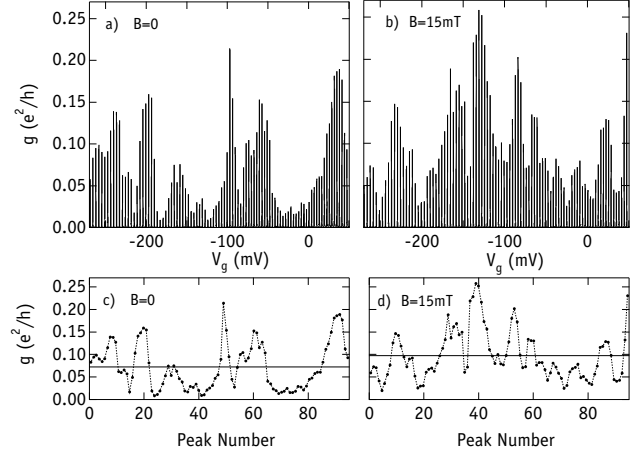


FIG. 1: Coulomb blockade peaks at electron temperature  $T_e = 45 \text{ mK}$ , for the  $0.7 \mu\text{m}^2$  device at (a)  $B = 0$  and (b)  $B = 15 \text{ mT}$ . Every second peak was measured, as peak-to-peak correlations made measuring each peak inefficient. (c,d) Peak heights, extracted from (a,b). Horizontal lines show average peak height, indicating suppression of average height at  $B = 0$ .

ventional weak localization, this effect changes the *average* conductance—or in the present context, the *average* CB peak height—upon breaking time-reversal symmetry with a weak magnetic field [11, 15].

At low temperatures, CB peak heights fluctuate considerably, as seen in Fig. 1, reflecting a distribution of tunneling strengths between the quantum modes in the dot and the leads. When  $\Gamma_1, \Gamma_2 \ll kT \ll \Delta$ , where  $\Gamma_{1(2)} = g_{1(2)}\Delta/2\pi$  are the couplings to the leads, transport occurs via a single eigenstate of the dot. In this case, CB peaks are thermally broadened and have a height  $g_o = (\pi/2kT)(\Gamma_1\Gamma_2/(\Gamma_1 + \Gamma_2))$  [16]. For chaotic or disordered dots, universal spatial statistics of wave functions allow full distributions of CB peak heights to be calculated for both broken ( $B \neq 0$ ) and unbroken ( $B = 0$ ) time-reversal symmetry [16, 17]. These distributions have been observed experimentally [18, 19], with good agreement between theory and experiment.

Although not emphasized in these earlier papers, it is readily seen that the two distributions have different averages. Introducing a dimensionless peak height  $\alpha = (1/\langle\Gamma\rangle)(\Gamma_1\Gamma_2/(\Gamma_1 + \Gamma_2))$  and assuming equivalent leads,  $\langle\Gamma_2\rangle = \langle\Gamma_1\rangle \equiv \langle\Gamma\rangle$ , one finds  $\langle\alpha\rangle_{B=0} = 1/4$  and  $\langle\alpha\rangle_{B \neq 0} =$

1/3. The resulting difference in average CB peak heights for the two distributions, normalized by the average peak height at  $B \neq 0$ ,

$$\delta\tilde{g}_o = \delta g_o / \langle g_o \rangle_{B \neq 0} = \frac{\langle g_o \rangle_{B \neq 0} - \langle g_o \rangle_{B=0}}{\langle g_o \rangle_{B \neq 0}}, \quad (1)$$

is then given by  $\delta\tilde{g}_o = (\langle \alpha \rangle_{B \neq 0} - \langle \alpha \rangle_{B=0}) / \langle \alpha \rangle_{B \neq 0} = 1/4$ . While the peak heights themselves are explicitly temperature dependent, this *normalized* difference,  $\delta\tilde{g}_o$ , does not depend on temperature in the absence of inelastic processes [11, 15].

The absence of explicit temperature dependence of  $\delta\tilde{g}_o$  is not limited to the regime  $kT \ll \Delta$ . As long as transport through the dot is dominated by elastic scattering ( $\Gamma_{el} \gg \Gamma_{in}$ , where  $\Gamma_{el} = (\Gamma_1 + \Gamma_2)$  is the broadening due to escape and  $\Gamma_{in}$  includes all inelastic processes), the normalized difference in averages does not change even for  $kT \gg \Delta$ , i.e., the result  $\delta\tilde{g}_o = 1/4$  is not affected by thermal averaging. This remains valid as long as  $kT < (E_{th}, E_c)$ , where  $E_{th} \sim \hbar/\tau_{cross}$  is the Thouless energy (inverse crossing time), and  $E_c$  is the charging energy of the dot.

As discussed in Ref. [11], the result  $\delta\tilde{g}_o = 1/4$  is reduced when inelastic processes dominate transport. In particular, when  $\Gamma_{el} \ll \Gamma_{in}$ ,  $\delta\tilde{g}_o(T) \rightarrow 0$  for  $kT_e/\Delta \rightarrow \infty$  (see Fig. 2(b)). The difference in temperature dependence of  $\delta\tilde{g}_o$  between  $\Gamma_{el} \ll \Gamma_{in}$  and  $\Gamma_{el} \gg \Gamma_{in}$  arises because for inelastic transport,  $\langle g_o \rangle \propto \langle \Gamma_1 \rangle \langle \Gamma_2 \rangle / (\langle \Gamma_1 \rangle + \langle \Gamma_2 \rangle)$  (the  $\Gamma$ 's are averaged individually), whereas for elastic transport,  $\langle g_o \rangle \propto \langle \Gamma_1 \Gamma_2 / (\Gamma_1 + \Gamma_2) \rangle$  (the entire fraction is averaged) [11]. It is this difference in behavior of  $\delta\tilde{g}_o(T)$  that we use to characterize the relative strength of inelastic processes.

Previous experiments investigating inelastic broadening of levels in nearly-isolated quantum dots have focused on relaxation of excited states, identifying a transition from a discrete to a continuous level spectrum at  $\epsilon > E_{th}$  [20, 21, 22]. Other experiments using coupled quantum dots have investigated phonon-mediated inelastic scattering between dots [23]. To our knowledge, the only experiment that has addressed the coherence of ground state transport in a single, nearly-isolated dot (i.e., at low bias,  $eV_{bias} < \Delta$ ) are the experiments of Yacoby *et al* [24] based on interference in an Aharonov-Bohm ring with a dot ( $N \sim 200$ ;  $\Delta \sim 40 \mu\text{eV}$ ) in one arm. Because interference around the ring was observed, the authors inferred a value  $\tau_\varphi > 10 \text{ ns}$  by assuming that the electron coherence time must be no shorter than the dwell time of an electron in the dot. This range for  $\tau_\varphi$  is somewhat longer than the values measured in open quantum dots using ballistic weak localization [4], suggesting that some enhancement of  $\tau_\varphi$  due to confinement may be occurring in the Yacoby experiment. However, since dot-in-ring measurements are rather different from weak-localization measurements, a direct comparison of values obtained in the two experiments may not be appropriate.

We report measurements for four different sized quantum dots formed in a two-dimensional electron gas

Area ( $\mu\text{m}^2$ )	$\Delta$ ( $\mu\text{eV}$ )	N	$E_{th}$ ( $\mu\text{eV}$ )	$E_c$ ( $\mu\text{eV}$ )	$\epsilon^{**}$ ( $\mu\text{eV}$ )
0.25	28	400	250	400	75
0.7	10	1400	150	290	32
3	2.4	6000	75	110	10
8	0.9	16000	45	65	5

TABLE I: Device parameters for the four quantum dots measured: dot area,  $A$ , assuming 100 nm depletion at edges; mean spacing of spin-degenerate levels,  $\Delta = 2\pi\hbar^2/m^*A$ , where  $m^*$  is the effective mass; number of electrons in the dot,  $N \sim nA$ , where  $n = 2 \times 10^{11} \text{ cm}^{-2}$  is the 2DEG density; Thouless energy,  $E_{th}$ ; charging energy  $E_{ch}$ ; and energy  $\epsilon^{**}$  below which dephasing times due to e-e interactions are predicted to diverge (see text).

(2DEG), defined using Cr-Au lateral depletion gates on the surface of a *GaAs/AlGaAs* heterostructure (see Table I). All dots were made from the same wafer, which has the 2DEG interface 90 nm below the surface and a Si doping layer 40 nm from the 2DEG. The electron density  $\sim 2.0 \times 10^{11} \text{ cm}^{-2}$  and bulk mobility  $\sim 1.4 \times 10^5 \text{ cm}^2/\text{Vs}$  yield a transport mean free path  $\sim 1.5 \mu\text{m}$ , larger than or comparable to the lithographic dimensions of the dots, making transport predominantly ballistic within the devices. Measurements were performed in a dilution refrigerator with base mixing chamber temperature of 25 mK. Electron temperature,  $T_e$ , in the reservoirs was measured directly using the width of CB peaks [25], indicating  $T_e = 45 \text{ mK}$  at base temperature.

CB peak heights were measured by sweeping one of the gate voltages,  $V_g$ , over many peaks while simultaneously trimming the gate voltages that control lead conductances to maintain a constant average transmission with balanced leads throughout the sweep. This allowed the collection of  $\sim 50$  peaks in the smallest dot, and hundreds of peaks in larger dots (see Fig. 1). Additional ensembles were then collected by making small changes to the dot shape using other gates. Average peak heights,  $\langle g_o \rangle$ , were extracted from these data, collected as a function of perpendicular magnetic field and normalized by their averages away from  $B = 0$ . Figure 2(a) shows that the functional form for the normalized average peak height,  $\langle \tilde{g}_o(B) \rangle = \langle g_o(B) \rangle / \langle g_o \rangle_{B \neq 0}$ , calculated within random matrix theory [15] agrees well with the experimental values. Note that the average peak height itself, dependent on temperature as well as the average lead transmissions, cannot be inferred from these normalized plots.  $\langle \tilde{g}_o(B) \rangle$  was measured at several temperatures in each device, and  $\delta\tilde{g}_o(T_e)$  was extracted for each. These are presented in Fig. 2(b), together with the predicted temperature dependences for  $\delta\tilde{g}_o(T_e)$  when either elastic or inelastic transport dominate [11]. Except where otherwise noted, the point contacts were set to give  $\langle g_o \rangle_{B \neq 0} \sim 0.05$ , though different dot shapes had average peak height that varied by up to 50%. The data in Fig. 2(b) represent averages over several ensembles at each temperature.

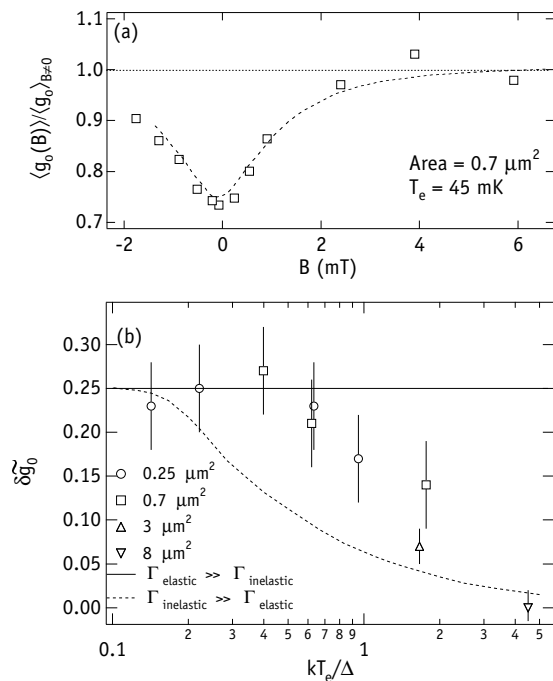


FIG. 2: (a) Average peak height as a function of perpendicular magnetic field, normalized by the average at  $B \neq 0$ , for the  $0.7 \mu\text{m}^2$  dot at  $T_e = 45 \text{ mK}$ . Theoretical curve (dashed) has one adjustable parameter, setting its width [15]. (b) Normalized change in average peak height at  $B = 0$ ,  $\delta\tilde{g}_0$ , at several temperatures,  $T_e$ , for all dots measured, along with theoretical values of  $\delta\tilde{g}_0$  when either elastic (solid curve) or inelastic (dashed curve) transport dominate [11]. Note crossover from solid to dashed curve around  $kT_e/\Delta \sim 1$ .

In the  $0.25 \mu\text{m}^2$  dot at  $T_e = 45 \text{ mK}$  and  $70 \text{ mK}$ ,  $\delta\tilde{g}_0$  was consistent with  $1/4$  as expected since  $kT_e \ll \Delta$  for both temperatures. In this regime, one cannot distinguish between elastic and inelastic scattering since both mechanisms give  $\delta\tilde{g}_0 \simeq 1/4$ . In the  $0.7 \mu\text{m}^2$  device at  $45 \text{ mK}$ , we again find  $\delta\tilde{g}_0 \sim 0.25$ . In this dot, however,  $45 \text{ mK}$  corresponds to  $kT_e/\Delta \sim 0.5$ . For  $\Gamma_{in} \gg \Gamma_{el}$ , a ratio  $kT_e/\Delta \sim 0.5$  gives a predicted value for the average peak height difference of  $\delta\tilde{g}_0 \sim 0.13$  (see the dashed curve in Fig. 2(b)) whereas for  $\Gamma_{el} \gg \Gamma_{in}$ ,  $\delta\tilde{g}_0 = 0.25$  for all values of  $kT_e/\Delta$  (solid line in Fig. 2(b)). We therefore conclude that  $\Gamma_{in} < \Gamma_{el}$  in the  $0.7 \mu\text{m}^2$  device at  $45 \text{ mK}$ , when the point contact transmissions are set so that  $\langle g_o \rangle \sim 0.05$ . We can extract  $\Gamma_{el}$  from average peak height  $\langle g_o \rangle$  using the equation  $\Gamma_{el} \sim \langle g_o \rangle \Delta$ , valid in the regime  $kT_e \gtrsim \Delta$  [16]. For  $\langle g_o \rangle \sim 0.05$  in the  $0.7 \mu\text{m}^2$  device, this gives  $\Gamma_{el} \sim 0.5 \mu\text{eV}$ , and we therefore conclude  $\Gamma_{in} < 0.5 \mu\text{eV}$  at  $45 \text{ mK}$ .

Similarly, we can observe for each dot (with different values of  $\Delta$ ), at each temperature, whether transport is principally elastic or inelastic, or whether the two rates are comparable. Measurements of  $\langle \tilde{g}_o(B) \rangle$  in the  $0.7 \mu\text{m}^2$  device at  $45 \text{ mK}$ ,  $70 \text{ mK}$ , and  $200 \text{ mK}$  are shown in Fig. 3, with the extracted values of  $\delta\tilde{g}_0(T)$  shown in the inset. For the  $0.7 \mu\text{m}^2$  device, we find that  $\Gamma_{el} > \Gamma_{in}$  at

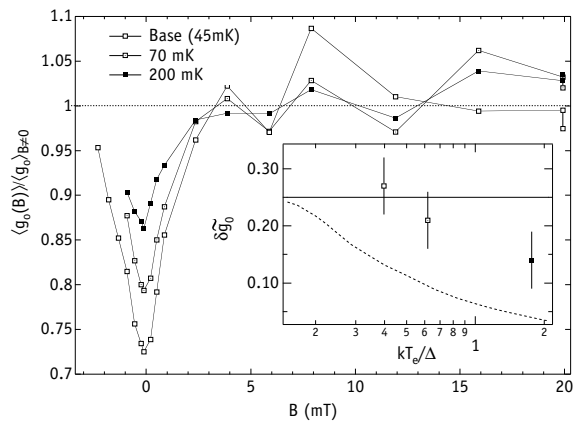


FIG. 3: (a) Normalized average peak height as a function of perpendicular magnetic field, for the  $0.7 \mu\text{m}^2$  dot at several temperatures. Inset shows  $\delta\tilde{g}_0$  for each temperature, along with theoretical curves from Ref. [11]. Note crossover from solid to dashed curve at  $T_e \sim 200 \text{ mK}$ .

$45 \text{ mK}$  and  $70 \text{ mK}$ , whereas by  $200 \text{ mK}$  the crossover to the lower curve ( $\Gamma_{el} < \Gamma_{in}$ ) has begun, presumably because  $\Gamma_{in}$  increases at higher temperature. We infer that a  $0.7 \mu\text{m}^2$  device at  $200 \text{ mK}$  is in the crossover regime  $\Gamma_{in} \sim 0.5 \mu\text{eV}$ .

We observe a similar crossover from  $\Gamma_{el} > \Gamma_{in}$  to  $\Gamma_{el} < \Gamma_{in}$  by changing  $\Gamma_{el}$  at fixed temperature. Figure 4 shows  $\langle \tilde{g}_o(B) \rangle$  in the  $0.7 \mu\text{m}^2$  device at  $200 \text{ mK}$  for three different settings of the point contacts, ranging from  $\langle g_o \rangle_{B \neq 0} = 0.016$  to  $\langle g_o \rangle_{B \neq 0} = 0.057$ ; the extracted values for  $\delta\tilde{g}_0$  are shown in the inset. Despite significant statistical uncertainty, it is clear that  $\delta\tilde{g}_0$  decreases as  $\Gamma_{el}$  decreases. We note that in the same device at  $45 \text{ mK}$  and  $70 \text{ mK}$  there is no difference in  $\delta\tilde{g}_0$  for the same of point contact transmissions, within experimental uncertainty. This is presumably because  $\Gamma_{in}$  is lower at these temperatures, and  $\Gamma_{el} > \Gamma_{in}$  for all point contact transmissions measured.

Based on recent theoretical arguments, one expects inelastic scattering due to electron-electron interactions to be strongly suppressed in isolated quantum dots for  $kT < \epsilon^{**}$ , where  $\epsilon^{**} \sim N^{1/4} \Delta$  for ballistic chaotic dots containing  $N$  electrons [8, 9, 10]. Because this suppression is not expected to occur in open dots, it is useful to compare the constraints on inelastic rates discussed above for nearly-isolated dots with experimental values of the phase coherence time  $\tau_\varphi$  measured in open dots [4]. Although there may be dephasing mechanisms that do not involve inelastic processes, the inelastic scattering rate should provide a lower bound for the dephasing rate  $\tau_\varphi^{-1}$ . Dephasing rates extracted from weak localization in open quantum dots are found to be well described by the empirical relation  $\hbar/\tau_\varphi(T_e) \sim 0.04 kT_e$  over the range of temperatures  $\sim 70 \text{ mK} - 300 \text{ mK}$ , independent of dot size [4]. For the closed dots we again may use  $\Gamma_{el} \sim \langle g_o \rangle \Delta$ , giving a ratio of elastic scattering rate to dephasing rate in the corresponding open dots

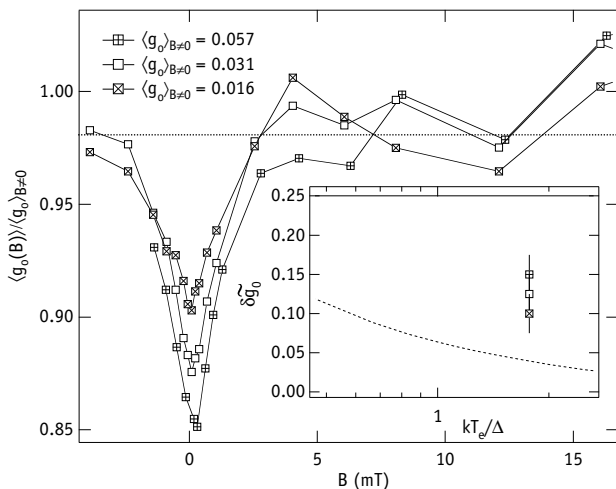


FIG. 4: (a) Normalized average peak height as a function of perpendicular magnetic field, for the  $0.7 \mu\text{m}^2$  dot at  $T_e = 200\text{mK}$  for three settings of the point contacts. Inset shows  $\delta \tilde{g}_0$  for setting, along with theoretical curves from Ref. [11]. As  $\Gamma_{in}$  is decreased by closing point contacts, experimental  $\delta \tilde{g}_0$  moves away from solid curve ( $\Gamma_{el} > \Gamma_{in}$ ) toward dashed curve ( $\Gamma_{el} < \Gamma_{in}$ ), as one would expect.

$\Gamma_{el}/(\hbar/\tau_\varphi) \sim (\langle g_0 \rangle / 0.04) kT_e/\Delta$ . If, for the sake of comparison, we identify  $\Gamma_{in}$  with  $\hbar/\tau_\varphi$ , we would then expect for  $\langle g_0 \rangle_{B \neq 0} \sim 0.05$  a ratio  $\Gamma_{el}/\Gamma_{in} \sim kT_e/\Delta$ , suggesting a crossover between the curves in Fig. 2(b) for  $kT_e/\Delta \sim 1$ . The data in Fig. 2(b) do show a crossover in the vicinity of  $kT_e/\Delta \sim 1$ , consistent with the identi-

fication  $\Gamma_{in}^{(closed)} \sim (\hbar/\tau_\varphi)^{(open)}$ . For a more quantitative comparison between dephasing in open dots and inelastic scattering through nearly-isolated dots, one would need a theoretical calculation of  $\delta \tilde{g}_0$  in the regime  $\Gamma_{el} \sim \Gamma_{in}$  [12].

We do not see evidence for the predicted [8, 9, 10] divergence of the coherence time for  $kT_e/\Delta < N^{1/4} \sim 5$ . A possible explanation is that electron-electron interactions are not the primary dephasing mechanism in our system. Several other mechanisms have been proposed, including external radiation [3, 26], two-level systems [27], and nuclear spins [28]. We cannot, however, rule out some enhancement of coherence due to confinement at a level reported in [24]. The lack of a quantitative theory in the crossover regime  $\Gamma_{in} \sim \Gamma_{el}$  prevents us from extracting exact values for  $\Gamma_{in}$  from our data.

In conclusion, we have developed a new method of measuring inelastic rates in a nearly-isolated quantum dot, using the change in average CB peak height upon breaking time-reversal symmetry. These measurements appear consistent with dephasing times previously measured in open ballistic quantum dots, however for a careful quantitative analysis of our data we await a theory treating the regime  $\Gamma_{in} \sim \Gamma_{el}$ .

We thank S. Patel for device fabrication and C. Duruöz for material growth. We acknowledge valuable discussions with I. Aleiner, Y. Alhassid, B. Altshuler, C. Beenakker, P. Brouwer, L. Glazman, and K. Held. This work was supported in part by the ARO under 341-6091-1-MOD 1 and DAAD19-99-1-0252. JAF acknowledges partial support from the DoD.

- 
- [1] P. Mohanty, E. M. Q. Jariwala, and R. A. Webb, Phys. Rev. Lett. **78**, 3366 (1997).  
[2] F. Pierre *et al.*, preprint (cond-mat/0012038), 2000.  
[3] B. L. Altshuler, M. E. Gershenson, and I. L. Aleiner, Physica E **3**, 58 (1998); M.E. Gershenson, Ann. Phys. **8**, 559, (1999).  
[4] A. G. Huibers *et al.*, Phys. Rev. Lett. **81**, 200 (1998); A. G. Huibers *et al.*, Phys. Rev. Lett. **83**, 5090 (1999).  
[5] U. Sivan, Y. Imry, and A. G. Aronov, Europhys. Lett. **28**, 115 (1994).  
[6] D. Loss and D. P. DiVincenzo, Phys. Rev. A **57**, 120 (1998).  
[7] G. Burkard, D. Loss, and D. P. DiVincenzo, Phys. Rev. B **59**, 2070 (1999).  
[8] B. L. Altshuler, Y. Gefen, A. Kamenev, and L. S. Levitov, Phys. Rev. Lett. **78**, 2803 (1997).  
[9] P. G. Silvestrov, Phys. Rev. Lett. **79**, 3994 (1997).  
[10] X. Leyronas, J. Tworzydło, and C. W. J. Beenakker, Phys. Rev. Lett. **82**, 4894 (1999).  
[11] C. W. J. Beenakker, H. Schomerus, and P. G. Silvestrov, preprint (cond-mat/0010387), 2000.  
[12] K. Held, I. L. Aleiner, B. L. Altshuler, in preparation.  
[13] B. L. Altshuler and A. G. Aronov, in *Electron-Electron Interaction in Disordered Systems*, eds. A. L. Efros and M. Pollak (Elsevier, Amsterdam, 1985).  
[14] G. Bergmann, Physics Reports **107**, 1 (1984).  
[15] Y. Alhassid, Phys. Rev. B **58**, 13383 (1998).  
[16] Y. Alhassid, Rev. Mod. Phys. **72**, 895 (2000).  
[17] R. A. Jalabert, A. D. Stone, and Y. Alhassid, Phys. Rev. Lett. **68**, 3468 (1992).  
[18] A. M. Chang *et al.*, Phys. Rev. Lett. **76**, 1695 (1996).  
[19] J. A. Folk *et al.*, Phys. Rev. Lett. **76**, 1699 (1996).  
[20] U. Sivan *et al.*, Europhys. Lett. **25**, 605 (1994).  
[21] D. C. Ralph, C. T. Black, and M. Tinkham, Phys. Rev. Lett., **78**, 4087 (1997).  
[22] D. Davidović and M. Tinkham, Phys. Rev. Lett. **83**, 1644 (1999).  
[23] T. Fujisawa *et al.*, Science **282**, 5390 (1998).  
[24] A. Yacoby, M. Heiblum, D. Mahalu, and H. Shtrikman, Phys. Rev. Lett. **74**, 4047 (1995).  
[25] L. P. Kouwenhoven *et al.*, in *Mesoscopic Electron Transport*, edited by L. L. Sohn, L. P. Kouwenhoven, and G. Schön (Kluwer, Dordrecht, 1997).  
[26] M. G. Vavilov and I. L. Aleiner, Phys. Rev. B **60**, 16311 (1999).  
[27] Y. Imry, H. Yukuyama, and P. Schwab, Europhys. Lett. **47**, 608 (1999); A. Zawadowski, J. vonDelft, and D. C. Ralph, Phys. Rev. Lett. **83**, 2632 (1999).  
[28] A. M. Dyugaev, I. D. Vagner, and P. Wyder, preprint (cond-mat/0005005), 2000.